Enhancement of Entanglement via Incoherent Collisions

Xihua Yang[1,*] Mingfei Cheng,[1] and Min Xiao[2,3,†]

[1]*Department of Physics and Institute for Quantum Science and Technology, Shanghai University, Shanghai 200444, China*
[2]*Department of Physics, University of Arkansas, Fayetteville, Arkansas 72701, USA*
[3]*National Laboratory of Solid State Microstructures and School of Physics, Nanjing University, Nanjing 210093, China*

(Received 13 July 2023; accepted 10 January 2024; published 8 February 2024)

In contrast to the general thought that the collisions are intrinsically dephasing in nature and detrimental to quantum entanglement at room or higher temperatures, here, we show that in the conventional ladder-type electromagnetically induced transparency (EIT) configuration, when the probe field intensity is not very weak as compared to the pump field, the entanglement between the bright pump and probe fields can be remarkably enhanced with the increase of the collisional decay rates in a moderate range in an inhomogeneously broadened atomic system. The strengthened entanglement results from the enhancement of constructive interference and suppression of destructive interference between one-photon and multi-photon transition pathways. Our results clearly indicate that the collisions offer a promising alternative to enhance entanglement at room or higher temperatures despite of the dephasing nature, which provides great convenience for experimental implementation, and opens new prospects and applications in realistic quantum computation and quantum information processing.

DOI: 10.1103/PhysRevLett.132.063601

It is generally thought that the collisions are dephasing in nature and detrimental to quantum coherence and interference as well as to squeezing and entanglement at room or higher temperatures. However, the collision-induced quantum effects have been extensively studied. The pressure-induced extra resonance resulted from collision-aided quantum interference was investigated first by Bloembergen in four-wave mixing (FWM) [1,2] and then by Grynberg in nonlinear spectroscopy [3]. The quantum interference between two collision-assisted excitation pathways has been demonstrated in both the frequency and time domains [4–6]. It was pointed out that the nature of quantum interference in the various three-level systems critically depends on the excitation scheme and the dephasing collisions can even change the nature [7,8]. Moreover, the control of coherent population transfer can be achieved via the collision-assisted electromagnetically induced transparency (EIT) and electromagnetically induced absorption (EIA) with the stimulated Raman adiabatic passage technique [9].

On the other hand, the generation of squeezing and entanglement only with the existence of suitable dephasing rates has also been investigated. It was shown that the realization of electromagnetically induced entanglement [10] and electromagnetically induced squeezing of atomic spin [11] would rely on suitable coherence decay rate of the lower doublet in the traditional Λ-type EIT configuration, and no squeezing or entanglement would exist with zero dephasing rate. This counterintuitive behavior has also been observed for the generation of pump-probe intensity correlation [12] and squeezed or entangled states of light [13,14] in the Λ-type coherent population trapping (CPT) or EIT configuration.

Motivated by the EIA via incoherent collisions in Ref. [8], we present a convenient and efficient way to enhance the bipartite entanglement between the bright pump and probe fields via incoherent collisions in the inhomogeneously broadened ladder-type atomic system. We show that when the probe field intensity is not very weak as compared to the pump field, the degree of the bipartite entanglement can be dramatically enhanced with the increase of the collisional decay rates in a moderate range due to the collision-assisted one-photon and multi-photon quantum interference. This method would greatly facilitate the generation and enhancement of bipartite entanglement between bright light fields at room or higher temperatures, and may find broad and potential applications in practical quantum information processing.

The considered ladder-type three-level atomic system driven by a strong coherent pump field and a relatively weak probe field denoted by the quantum operators a_2 and a_1, is shown in Fig. 1(a), where the levels 1, 2, and 3 correspond, respectively, to the levels $5S$ $(F=3)$, $5P_{3/2}$, and $5D_{5/2}$ of the ^{85}Rb atom. The probe (pump) field with frequency ω_1 (ω_2) couples the levels 1 and 2 (levels 2 and 3) with the frequency detuning $\Delta_1 = \omega_1 - \omega_{21}$ ($\Delta_2 = \omega_2 - \omega_{32}$). We denote $2\gamma_1$ ($2\gamma_2$) as the population decay rates from level 2 to level 1 (level 3 to level 2), and γ_{ij} ($i \neq j$) as the coherence decay rate between levels i and j. Apart from the radiative relaxation, the atoms also undergo collisions, and the collision-induced coherence decay rate

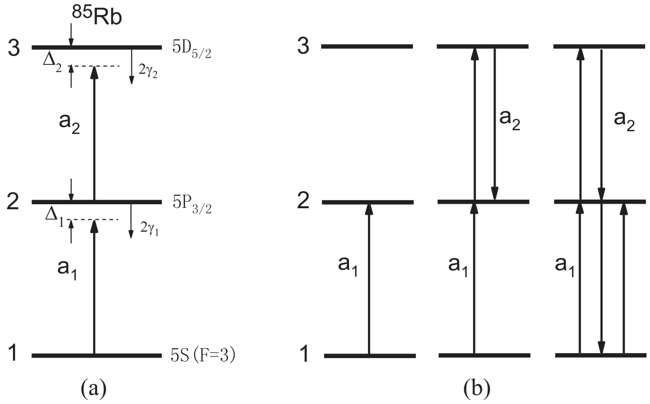

FIG. 1. (a) The ladder-type three-level atomic system driven by a strong coherent pump field (a_2) and a relatively weak probe field (a_1), where levels 1, 2, and 3 correspond, respectively, to the levels $5S$ ($F=3$), $5P_{3/2}$, and $5D_{5/2}$ of the ^{85}Rb atom. (b) The one-photon, three-photon, and five-photon excitation processes for the probe field absorption.

between levels i and j is denoted by γ_{ijp} ($i \neq j$). In what follows, we take into account the quantum features of both the pump and probe fields, and examine the bipartite entanglement between the two bright light fields in the inhomogeneously broadened ladder-type atomic system under different collisional damping rates.

The interaction Hamiltonian of the system in the rotating-wave approximation has the form [15–17],

$$\hat{V} = -\frac{\hbar N}{L}\int_0^L dz\big[\Delta_1\sigma_{22}(z,t) + (\Delta_1+\Delta_2)\sigma_{33}(z,t) + g_1a_1(z,t)\sigma_{21}(z,t) + g_2a_2(z,t)\sigma_{32}(z,t) + \mathrm{H.c.}\big], \quad (1)$$

where N is the total number of atoms in the interaction volume, $g_{1(2)} = \mu_{12(23)}\varepsilon_{1(2)}/\hbar$ is the atom-field coupling constant with $\mu_{12(23)}$ being the dipole moment for the 1–2 (2–3) transition, and $\varepsilon_{1(2)} = \sqrt{\hbar\omega_{1(2)}/2\epsilon_0 V}$ being the electric field of a single probe (pump) photon, ϵ_0 is the free space permittivity, and V is the interaction volume with length L and beam radius r. The Heisenberg-Langevin equations and the coupled propagation equations are similar to those in Ref. [10], except that the two fields are applied in the counterpropagating configuration so as to eliminate the two-photon Doppler effect for the present case.

As is well known, the successful generation of entanglement using initially coherent light fields in an atomic system critically relies on the strong nonlinear interaction (e.g., FWM process) of light fields with atoms. In fact, FWM has proven to be an efficient process to produce entanglement, as demonstrated by the generation of entangled Stokes and anti-Stokes photons in the Λ-type atomic system [18–25]. With this in mind, and based on the collision-induced EIA in Ref. [8], we try to test the bipartite entanglement between the pump and probe fields with comparable intensity under different collisional decay rates shown in Fig. 1(a). With the similar analysis to that in Refs. [8,26,27], considering the two-step two-photon excitation (TSTPE) as the dominant contribution to the probe absorption for the higher-order terms of the probe field, we solve the Heisenberg-Langevin equations iteratively to the fifth order of the mean value of the collective atomic operators $\langle\sigma_{21}\rangle$, and get the expression for the probe absorption coefficient with the consideration of the Doppler broadening to be

$$\alpha(\Delta_1) \propto \frac{\gamma_{21}}{g_1\langle a_1\rangle}\int dvD(v)\mathrm{Im}\langle\sigma_{21}\rangle = \int dvD(v)\left\{\frac{\gamma_{12}^2}{\gamma_{12}^2+\Delta_1^2} - \mathrm{Re}\left[\frac{\gamma_{12}(g_2\langle a_2\rangle)^2}{(\gamma_{12}+j\Delta_1)^2[\gamma_{13}+j(\Delta_1+\Delta_2)]}\right] + \frac{(g_1\langle a_1\rangle)^2(g_2\langle a_2\rangle)^2}{4\gamma_1\gamma_2\gamma_{12}\gamma_{23}}\frac{\gamma_{23}^2}{\gamma_{23}^2+\Delta_2^2}\left(\frac{\gamma_{12}^2}{\gamma_{12}^2+\Delta_1^2}\right)^2\right\}, \quad (2)$$

where $D(v) = \exp(-v^2/\mu^2)/(\sqrt{\pi}\mu)$ is the normalized Doppler distribution with μ being the root-mean-square atomic velocity. It can be seen clearly that Eq. (2) is essentially the same as that in Refs. [8,26,27], only with $g_1\langle a_1\rangle$ and $g_2\langle a_2\rangle$ replaced by their Rabi frequencies in the semiclassical density-matrix approach.

The entanglement feature of the pump and probe fields with comparable intensity under different collisional dephasing rates can be intuitively understood in terms of the nonlinear interaction between the laser fields and atoms shown in Fig. 1(b). The one-photon and multiphoton excitation processes presented in Fig. 1(b) can be well described by the three components in Eq. (2) for the probe absorption. The first term comes from the traditional one-photon linear absorption; the second is from the lowest-order term in the pump field, which is the origin of EIT; and the third term consists of a five-photon process, representing the TSTPE. Clearly, both of the nonlinear processes EIT and TSTPE have contributions to the generation of the entanglement between the pump and probe fields. As discussed in Ref. [10], the EIT process is essentially a FWM process, which can be equivalently regarded as a closed-loop light-atom interaction, and in the present scheme, the FWM process involves the absorption of one probe photon and one pump photon and subsequent emission of one pump photon and one probe photon. Since every probe photon absorption (emission) is always accompanied by absorbing (emitting) one pump photon, strong quantum correlation and entanglement between the pump and probe fields can be produced. In the same way, the TSTPE process is essentially a six-wave mixing (SWM) process, involving the simultaneous absorption (emission) of one probe photon and one pump photon as well as the absorption of another probe photon accompanied by the emission of a further probe photon, which can also lead to strong quantum correlation and entanglement between the pump and probe fields.

However, as seen from Eq. (2), the second term has a minus sign with respect to the first term, and the destructive interference between the one-photon and three-photon transition pathways results in EIT, which would trap atoms in the level 1; subsequently, the FWM process as well as the bipartite entanglement would be weakened due to the EIT-induced reduction of population transfer, and even no entanglement would exist if the dephasing rate γ_{13} were zero, as evidenced in the Λ-type three-level atomic system in Ref. [10]. On the contrary, the TSTPE term has the same sign as the first term, and the constructive interference between the one-photon and five-photon transition pathways results in EIA, which would strengthen the SWM process as well as the bipartite entanglement between the pump and probe fields with comparable intensity. Moreover, as analyzed in Ref. [8], the EIT term would decrease much more quickly than the TSTPE term with increasing the collisional decay rates due to the collisional decay rate γ_{13p} equal to the sum of γ_{12p} and γ_{23p}. This would lead to the change of the probe field absorption at the two-photon resonance from EIT to EIA, and subsequent enhancement of the bipartite entanglement with the increase of the collisional decay rates in a moderate range.

The above prediction is confirmed by solving the Heisenberg-Langevin equations and coupled propagation equations for the interaction of the two fields with atoms. We use the similar analysis to that in Ref. [28] by writing each atomic or field operator as the sum of its mean value and a quantum fluctuation term to treat the atom-field interaction. We consider the case that $g_2\langle a_2\rangle$ is larger than $\sqrt{\gamma_{12}\gamma_{13}}$, so the depletions of the pump and probe fields can be safely neglected. To take into account the Doppler broadening, we assume the number of atoms per unit volume with velocity v is $N(v)$ with the velocity distribution traditionally taken to be Maxwellian, and their contributions to the total atomic operators are obtained by integrating over the velocity distribution. Instead of using the criterion proposed by Duan *et al.* [29] (a sufficient criterion), we employ the necessary and sufficient criterion, i.e., the positive partial transposition criterion, which is stated in terms of the symplectic eigenvalues of the partially transposed covariance matrix $\tilde{\sigma}$ [30,31], to test entangled properties of the pump and probe fields. The symplectic eigenvalues can be computed as the absolute value of the eigenvalues of $i\Omega\tilde{\sigma}$ with $\Omega = \left(\begin{smallmatrix}1&0\\0&1\end{smallmatrix}\right) \otimes \left(\begin{smallmatrix}0&1\\-1&0\end{smallmatrix}\right)$, and the degree of the bipartite entanglement can be quantified by the smallest symplectic eigenvalue V_{12} [32]. If V_{12} is smaller than 1, then genuine bipartite entanglement is present, and the smaller V_{12} is, the higher the degree of the bipartite entanglement becomes. In the following, we assume the probe and pump fields to be initially in the coherent states $|\alpha_1\rangle$ and $|\alpha_2\rangle$, and the relevant parameters are scaled with m and MHz and set according to the realistic experimental conditions [33] with $r = 4.5\times10^{-4}$, $L = 0.006$, $\gamma_1 = 3$, $\gamma_2 = 0.5$, the atomic saturation density $n_0 = 8.5\times10^{15}$, and Doppler-broadened width $\Delta_w = 530$ at room temperature.

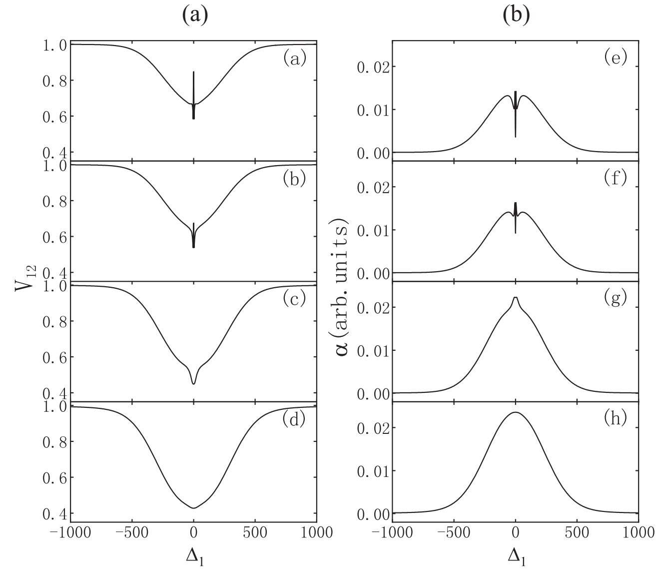

FIG. 2. The dependences of V_{12} at zero Fourier frequency (column A) and the probe absorption coefficient α (column B) with the Doppler-broadening average on the probe field detuning Δ_1 with $\Delta_2 = 0$ $r = 4.5\times10^{-4}$, $L = 0.006$, $\gamma_1 = 3$, $\gamma_2 = 0.5$, $\alpha_2 = 5\alpha_1 = 50$, $n_0 = 8.5\times10^{15}$, $\Delta_w = 530$, $\gamma_{12p} = \gamma_{23p} = 1p$, and $\gamma_{13p} = \gamma_{12p} + \gamma_{23p} = 2p$ (p represents the relative collisional decay rate) under different collisional decay rates $p = 0$ (a),(e), $p = 0.5$ (b),(f), $p = 6$ (c),(g), and $p = 20$ (d),(h), respectively.

Figure 2 gives the main result of this study, where the smallest symplectic eigenvalue V_{12} at zero Fourier frequency and the probe absorption coefficient α with the Doppler-broadening average as a function of the probe field detuning Δ_1 under different collisional decay rates $\gamma_{\rm ijp}$ are depicted on the left column (A) and right column (B), respectively. Here, p represents the relative collisional decay rate, which can be easily controlled by adding buffer gas (e.g., Ne or Ar as in Refs. [4,6]) into the cell. It can be seen from the right column (B) that, similar to the results in Ref. [8], the line shape of the probe field absorption is changed from EIT to EIA with the increase of $\gamma_{\rm ijp}$ in a moderate range. The most interesting thing is that on the left column (A), the evolution of V_{12} almost exhibits an inverse behavior as compared to the probe absorption spectra. When there are no dephasing collisions [see $p = 0$ in Fig. 2(a)], V_{12} is always smaller than 1 in the whole Doppler-broadened range of the probe field detuning, which demonstrates the generation of genuine bipartite entanglement between the pump and probe fields, and its line shape is a superposition of a sharp inverted dip with two narrow inverted peaks on its two sides superimposed on the inverted Doppler-broadened background, which results from the combination of EIT and TSTPE processes. However, the generated bipartite entanglement at the two-photon resonance is relatively weak due to the EIT effect. With the increase of $\gamma_{\rm ijp}$, the line shape of V_{12} would change from a narrow inverted dip into a distinct narrow inverted peak [see Figs. 2(a)–2(c)]. When $\gamma_{\rm ijp}$ is increased to the order of the pump field Rabi frequency, a widely broadened profile with a smaller reduction of V_{12} is obtained. Obviously, dramatic enhancement of the entanglement can be achieved via incoherent collisions in a moderate range. Further calculations show that the inverted narrow entanglement peak in Fig. 2(c) moves according to the pump field detuning and just stands where the condition for the two-photon resonance is fulfilled, which clearly demonstrates that the entanglement peak in Fig. 2(c) does result from the collision-assisted one-photon and multi-photon quantum interference.

Figures 3(a) and 3(b) depict the dependences of V_{12} and α on the pump field amplitude α_2 for the cases $p = 0$ and $p = 20$. In this case, in order to keep the mean values of atomic operators and intensity absorption rates of the two fields nearly stable so as to compare the degrees of entanglement under different field intensities, as done in Ref. [10], the ratios of α_2/α_1, $\gamma_{12,13,23}/\alpha_1$, and n/α_1 are kept fixed. As seen in Fig. 3(a), nearly no entanglement would occur for both cases of $p = 0$ and $p = 20$ when the pump field is relatively weak. With the increase of α_2, there would exist an optimal pump field intensity for achieving the strongest entanglement. This is due to the fact that, on one hand, the bipartite entanglement results from the nonlinear interaction between the atoms and laser fields, which would be enhanced with increasing the pump and probe field intensities; on the other hand, as shown in Fig. 3(b), the probe field absorption would decrease with increasing α_2, that is, the EIT effect would be strengthened, which would trap the atoms in the level 1 and deteriorate the generation of entanglement. The optimal pump field intensity for the maximal degree of entanglement occurs when the effects of the two nonlinear processes balances each other. This can be further demonstrated by employing a stronger pump field ($\alpha_2 = 30\alpha_1$) with $p = 6$ in Figs. 3(c) and 3(d), where the narrow inverted entanglement peak in Fig. 2(c) turns into an inverted dip in Fig. 3(c), and the narrow probe absorption peak in Fig. 2(g) turns into a dip in Fig. 3(d). It is clear that the degree of bipartite entanglement would be dramatically reduced at the two-photon resonance due to the stronger EIT effect associated with the higher pump field intensity.

In order to be more conducive to guiding the experiment, we present the dependences of V_{12} at zero Fourier frequency and α on the probe field amplitude α_1 with fixed $\alpha_2 = 50$ in Figs. 4(a) and 4(b) and on the relative collisional decay rate p in Figs. 4(c) and 4(d). It can be seen from Fig. 4(a) that there also exists an optimal probe field

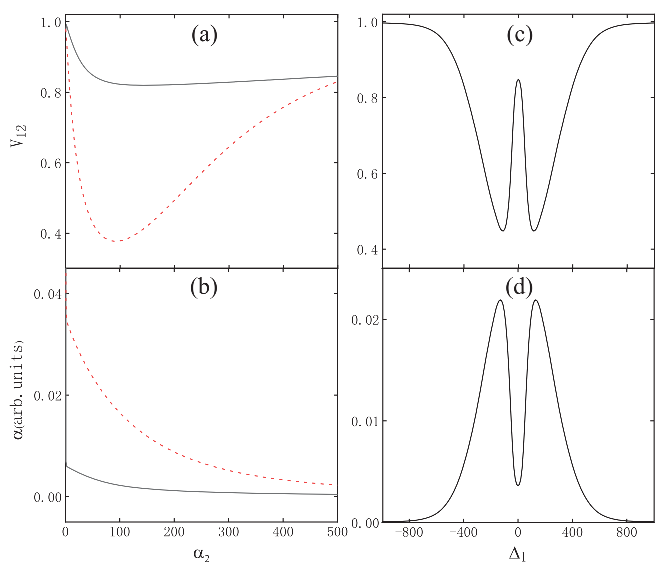

FIG. 3. The dependences of V_{12} at zero Fourier frequency (a),(c) and α (b),(d) on the pump field amplitude α_2 for the cases $p = 0$ (solid black lines) and $p = 20$ (dashed red lines) with $\Delta_1 = 0$, $\alpha_2 = 5\alpha_1$, $n = n_0\alpha_1/10$, and $\gamma_{12,13,23}$ replaced by $\gamma_{12,13,23}\alpha_1/10$ (a),(b) and on the probe field detuning Δ_1 with $p = 6$, $\alpha_2 = 30\alpha_1$ (c),(d), and the other parameters are the same as those in Fig. 2.

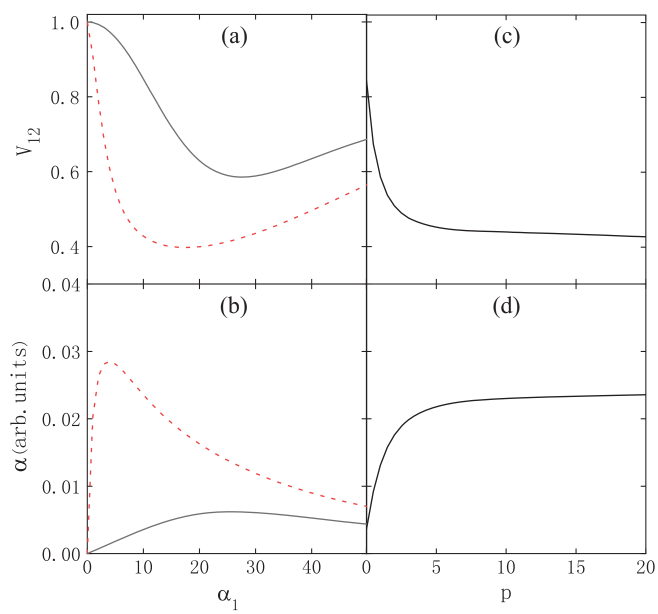

FIG. 4. The dependences of V_{12} at zero Fourier frequency (a),(c) and α (b),(d) on α_1 with fixed $\alpha_2 = 50$ for the cases $p = 0$ (solid black lines) and $p = 20$ (dashed red lines) (a),(b) and on p (c),(d) with $\Delta_1 = 0$, and the other parameters are the same as those in Fig. 2.

amplitude for achieving a maximal degree of entanglement for both $p = 0$ and $p = 20$, and apparent entanglement enhancement can be obtained with the amplitude ratio α_1/α_2 in a moderate range ($0.1 \sim 0.3$). Note that the decrease of probe absorption with further increasing α_1 in Fig. 4(b) results from the nonlinear interaction between the two strong fields and atoms, exhibiting the analog of CPT in the Λ-type system. Moreover, as shown in Figs. 4(c) and 4(d), V_{12} is almost decreased from 0.85 to 0.43 with the variation of p from 0 to 20, accompanied by the increase of the probe field absorption. Obviously, remarkable enhancement of entanglement can be realized with increasing the collisional decay rates within a reasonable range that the depletions of the pump and probe fields can be safely neglected.

In realistic experiments, the collisional decay rates critically depend on both the added buffer gas pressure and sample temperature, which can be easily controlled by changing the buffer gas pressure in the cell, whereas the total atomic number in the interaction volume (proportional to the atomic density) would increase apparently with the increase of the temperature. In order to successfully observe the entanglement enhancement via incoherent collisions, a suitable temperature and buffer gas pressure should be employed; too high temperature and/or buffer gas pressure would lead to the breakdown of the approximation of neglecting the depletions of the pump and probe fields, which may result in the weakness and even disappearance of entanglement. For example, experimental conditions with the pump and probe field powers of about tens of milliwatts and Ne or Ar buffer gas pressure of several torr at room temperature, may satisfy the parameters used for Fig. 2(c). Since the absorption rate of the two fields would display an exponential increase with respect to the total atomic number in the interaction volume, one feasible way for observing this effect at higher temperatures can be achieved by adding limited Rb atoms into the cell, thereby keeping the atomic density smaller than its saturation density and the total atomic number in the interaction volume nearly fixed, which is far superior to those using cold atoms for experimental implementation [34–36].

In conclusion, we have demonstrated the enhancement of entanglement between two bright light fields via incoherent collisions in the traditional inhomogeneously broadened ladder-type atomic system. The strengthened entanglement results from the enhancement of constructive interference and suppression of destructive interference between one-photon and multiphoton transition pathways with the increase of the collisional decay rates in a moderate range. This method provides a promising alternative to generate and enhance nondegenerate continuous-variable entanglement between two bright light beams via incoherent collisions at room or higher temperatures, and may find potential applications in practical quantum information processing protocols.

This work is supported by National Natural Science Foundation of China (No. 12174243).

*yangxh@shu.edu.cn
†mxiao@uark.edu

[1] N. Bloembergen, *Laser Spectroscopy IV*, edited by H. Walther and K. W. Rothe (Springer, Berlin, 1979), p. 340.
[2] Y. Prior, A. R. Bogdan, M. Dagenais, and N. Bloembergen, Phys. Rev. Lett. **46**, 111 (1981).
[3] G. Grynberg and P. R. Berman, Phys. Rev. A **41**, 2677 (1990).
[4] X. H. Yang and H. K. Xie, Phys. Rev. A **67**, 063807 (2003).
[5] X. H. Yang, Z. R. Sun, S. A. Zhang, L. E. Ding, and Z. G. Wang, J. Phys. B **38**, 2519 (2005).
[6] X. H. Yang, Z. R. Sun, and Z. G. Wang, Phys. Rev. A **76**, 043417 (2007).
[7] G. S. Agarwal, Phys. Rev. A **55**, 2467 (1997).
[8] X. H. Yang, J. T. Sheng, and M. Xiao, Phys. Rev. A **84**, 043837 (2011).
[9] X. H. Yang and S. Y. Zhu, Phys. Rev. A **78**, 023818 (2008).
[10] X. H. Yang and M. Xiao, Sci. Rep. **5**, 13609 (2015).
[11] X. H. Yang, X. P. Shao, and M. F. Chen, J. Mod. Opt. **66**, 1071 (2019).
[12] P. Barberis-Blostein and N. Zagury, Phys. Rev. A **70**, 053827 (2004).
[13] F. A. M. de Oliveira, B. J. Dalton, and P. L. Knight, J. Opt. Soc. Am. B **4**, 1558 (1987).
[14] Y. L. Chuang, R. K. Lee, and I. A. Yu, Opt. Express **29**, 3928 (2021).
[15] M. Fleischhauer, Phys. Rev. Lett. **72**, 989 (1994).
[16] P. Kolchin, Phys. Rev. A **75**, 033814 (2007).
[17] Q. Glorieux, R. Dubessy, S. Guibal, L. Guidoni, J. P. Likforman, T. Coudreau, and E. Arimondo, Phys. Rev. A **82**, 033819 (2010).
[18] L. M. Duan, M. D. Lukin, J. I. Cirac, and P. Zoller, Nature (London) **414**, 413 (2001).
[19] C. H. van der Wal, M. D. Eisaman, A. André, R. L. Walsworth, D. F. Phillips, A. S. Zibrov, and M. D. Lukin, Science **301**, 196 (2003).
[20] A. Kuzmich, W. P. Bowen, A. D. Boozer, A. Boca, C. W. Chou, L. M. Duan, and H. J. Kimble, Nature (London) **423**, 731 (2003).
[21] M. D. Lukin, P. R. Hemmer, and M. O. Scully, Adv. At. Mol. Opt. Phys. **42**, 347 (2000).
[22] V. Balic, D. A. Braje, P. Kolchin, G. Y. Yin, and S. E. Harris, Phys. Rev. Lett. **94**, 183601 (2005).
[23] V. Boyer, A. M. Marino, R. C. Pooser, and P. D. Lett, Science **321**, 544 (2008).
[24] A. M. Marino, R. C. Pooser, V. Boyer, and P. D. Lett, Nature (London) **457**, 859 (2009).
[25] X. Yang, Y. Zhou, and M. Xiao, Phys. Rev. A **85**, 052307 (2012).
[26] S. Wielandy and A. L. Gaeta, Phys. Rev. A **58**, 2500 (1998).
[27] N. Hayashi, A. Fujisawa, H. Kido, K. Takahashi, and M. Mitsunaga, J. Opt. Soc. Am. B **27**, 1645 (2010).
[28] L. Davidovich, Rev. Mod. Phys. **68**, 127 (1996).
[29] L. M. Duan, G. Giedke, J. I. Cirac, and P. Zoller, Phys. Rev. Lett. **84**, 2722 (2000).
[30] R. Simon, Phys. Rev. Lett. **84**, 2726 (2000).
[31] R. F. Werner and M. M. Wolf, Phys. Rev. Lett. **86**, 3658 (2001).

[32] K. Zhang, W. Wang, S. S Liu, X. Z Pan, J. J. Du, Y. B. Lou, S. Yu, S. C. Lv, N. Treps, C. Fabre, and J. T. Jing, Phys. Rev. Lett. **124**, 090501 (2020).
[33] Y. P. Zhang, B. Anderson, and M. Xiao, Phys. Rev. A **77**, 061801(R) (2008).
[34] I. Bloch, Nature (London) **453**, 1016 (2008).
[35] P. Kunkel, M. Prüfer, H. Strobel, D. Linnemann, A. Frölian, T. Gasenzer, M. Gärttner, and M. K. Oberthaler, Science **360**, 413 (2018).
[36] X. J. Wang, S. J. Yang, P. F. Sun, B. Jing, J. Li, M. T. Zhou, X. H. Bao, and J. W. Pan, Phys. Rev. Lett. **126**, 090501 (2021).